

Symmetry energy effects on location of the inner edge of neutron star crusts

Ch C Moustakidis^{1,2*}

¹*Department of Theoretical Physics,
Aristotle University of Thessaloniki, 54124 Thessaloniki, Greece*

²*Theoretical Astrophysics, University of Tuebingen IAAT,
Auf der Morgenstelle 10, Tuebingen 72076 Germany*

Abstract

The symmetry energy effects on the location of the inner edge of neutron star crusts are studied. Three phenomenological models are employed in order to check the accuracy of the well known parabolic approximation of the equation of state for asymmetric nuclear matter in the determination of the transition density n_t and transition pressure P_t . The results corroborate the statement that the error due to the assumption that a priori the equation of state is parabolic may introduce a large error in the determination of related properties of a neutron star as the crustal fraction of the moment of inertia and the critical frequency of rotating neutron stars.

PACS number(s): 21.65.cd, 21.65.Ef, 21.65.Mn, 26.60.Kp, 26.60.-c, 26.60.Gj.

Keywords: Equation of state; nuclear symmetry energy; neutron star crust.

*Electronic address: moustaki@auth.gr

I. INTRODUCTION

Neutron stars (NS) are extraordinary astronomical laboratories for the physics of dense neutron-rich nuclear matter [1, 2]. The main parts of a NS are the crust and the core. The latter, divided into the outer core and the inner one, has a radius of approximately 10 km and contains most of the star's mass while the crust, with a thickness of about 1 km and containing only a few percent of the total mass, can also be divided into an outer and an inner part. A very important ingredient in the study of the structure and various properties of neutron stars is the equation of state (EOS) of neutron-rich nuclear matter [3].

One of the most important predictions of a given EOS is the location of the inner edge of a neutron star crust. The inner crust comprises the outer region from the density at which neutrons drip-out of nuclei, to the inner edge separating the solid crust from the homogeneous liquid core. At the inner edge, in fact, a phase transition occurs from the high-density homogeneous matter to the inhomogeneous one at lower densities. The transition density takes its critical value n_c when the uniform neutron-proton-electron matter (npe) becomes unstable with respect to the separation into two coexisting phases (one corresponding to nuclei, the other one to a nucleonic sea) [3].

While the density at which neutrons drip-out of nuclei is rather well determined, the transition density n_t at the inner edge is much less certain due to our insufficient knowledge of the EOS of neutron-rich nuclear matter. The value of n_t determines the structure of the inner part of the crust. If sufficiently high, it is possible for non-spherical phases, with rod- or plate-like nuclei, to occur before the nuclei dissolve. If n_t is relatively low, then the matter undergoes a direct transition from spherical nuclei to uniform nucleonic fluid. The extent to which non-spherical phases occur will have important consequences for other properties determined by the solid crust [4].

In general, the determination of the transition density n_t itself is a very complicated problem because the inner crust may have a very complicated structure. A well established approach is to find the density at which the uniform liquid first becomes unstable against small-amplitude density fluctuations, indicating the formation of nuclear clusters. This approach includes the dynamical method [4–12], the thermodynamical one [3, 13–15], and the random phase approximation (RPA) [16, 17].

Theoretical studies have shown that the core-crust transition density and pressure are very sensitive to the density dependence of the nuclear matter symmetry energy [3, 11–22]. At present, the symmetry energy is well constrained experimentally up to the value of the nuclear saturation density n_0 but still remains almost unknown in the density regime appropriate for the interior of neutron stars ($n \gg n_0$) [23–25]. In spite of the experimental uncertainty of the symmetry energy, there are many theoretical considerations of the symmetry energy categorized mainly in phenomenological and effective field theoretical approaches. The aim of this work is: a) to apply a momentum dependent interaction model (MDI) as well as two additional non relativistic models (Thomas-Fermi and Skyrme type) to determine the transition density and transition pressure corresponding to the edge of a neutron star crust and b) to check the accuracy of the parabolic approximation widely used in the literature and applied to neutron star research.

The article is organized as follows. In Sec. 2 we review the Taylor expansion of the energy while in Sec. 3 we present the thermodynamical method for the determination of the transition density and pressure of the inner edge of a neutron star crust. The nuclear models employed in the the present work are presented in Sec. 4. The results are presented and discussed in Sec. 5. Finally Sec. 6 summarizes the present study.

II. TAYLOR EXPANSION OF THE ENERGY

The energy per particle $E(n, I)$ in cold asymmetric nuclear matter can be expanded around $I = 0$ as follows

$$E(n, I) = E(n, I = 0) + E_{sym,2}(n)I^2 + E_{sym,4}(n)I^4 + \dots + E_{sym,2k}(n)I^{2k} + \dots, \quad (1)$$

where the total baryon density $n = n_p + n_n$, n_p (n_n) is the proton (neutron) density, $I = (n_n - n_p)/n$ is the asymmetry parameter and $E(n, I = 0)$ is the energy per baryon of the symmetric nuclear matter, while the coefficients of the expansion are

$$\begin{aligned} E_{sym,2}(n) &= \frac{1}{2!} \frac{\partial^2 E(n, I)}{\partial I^2} \Big|_{I=0}, & E_{sym,4}(n) &= \frac{1}{4!} \frac{\partial^4 E(n, I)}{\partial I^4} \Big|_{I=0}, \\ E_{sym,2k}(n) &= \frac{1}{(2k)!} \frac{\partial^{2k} E(n, I)}{\partial I^{2k}} \Big|_{I=0}. \end{aligned} \quad (2)$$

In (1), only even powers of I appear due to the fact that the strong interaction must be symmetric under exchange of neutrons with protons i.e. the contribution to the energy must

be independent of the sign of the difference $n_n - n_p$. The second order approximation of the expansion (1) is written as

$$E(n, I) \simeq E(n, I = 0) + E_{sym,2}(n)I^2. \quad (3)$$

We expect, from a mathematical point of view, that the above expansion is accurate at least close to $I = 0$ (the case of symmetric nuclear matter). However for the majority of the energy functionals, the above approximation works well for higher values of the asymmetry parameter I and even close to the value $I = 1$ corresponding to the pure neutron matter. Thus, in cases for which the expansion, in a good approximation, is independent of the asymmetry parameter I , the symmetry energy can be defined as

$$E_{sym}(n) = E(n, I = 1) - E(n, I = 0), \quad (4)$$

and the energy per baryon is written

$$E(n, I) = E(n, I = 0) + \underbrace{(E(n, I = 1) - E(n, I = 0))}_{E_{sym}(n)} I^2. \quad (5)$$

The knowledge of the equation of state of neutron rich matter is fundamental in astrophysical applications. For example it is the basic ingredient for the study of β -stable matter characteristic for the interior of neutron stars. Actually, for the most of the equations of state (mainly those originating from microscopic calculations or those coming from relativistic mean field theories) only the energy of symmetric nuclear matter and pure neutron matter are determined and the definition of the symmetry energy from equation (4) is almost unavoidable. The question naturally arising is the magnitude of the width of the error introduced by assuming a priori that the equation of state is parabolic according to relations (1) and (5).

In the present work we define in addition the *second order expansion* of the form

$$E(n, I) \simeq E(n, I = 0) + E_{sym,2}(n)I^2 = E(n, I = 0) + \frac{1}{2!} \frac{\partial^2 E(n, I)}{\partial I^2} \Big|_{I=0} I^2, \quad (6)$$

which is similar to expansion (5) replacing the quantity $E_{sym}(n) = E(n, I = 1) - E(n, I = 0)$ by $E_{sym,2}(n) = \frac{1}{2!} \frac{\partial^2 E(n, I)}{\partial I^2} \Big|_{I=0}$.

Before trying to check the accuracy of the approximation (5) it is worth to compare the density dependence of the above two definitions of the symmetry energy i.e. $E_{sym,2}(n)$ and $E_{sym}(n)$ given by (2) and (4) respectively.

III. THE THERMODYNAMICAL METHOD

The core-crust interface corresponds to the phase transition between nuclei and uniform nuclear matter. The uniform matter is nearly pure neutron matter, with a proton fraction of just a few percent determined by the condition of beta equilibrium. Weak interactions conserve both baryon number and charge [3], and from the first law of thermodynamics, at temperature $T = 0$ we have

$$du = -Pdv - \hat{\mu}dq, \quad (7)$$

where u is the internal energy per baryon, P is the total pressure, v is the volume per baryon ($v = 1/n$ where n is the baryon density) and q is the charge fraction ($q = x - Y_e$ where x and Y_e are the proton and electron fractions in baryonic matter respectively). In β -equilibrium the chemical potential $\hat{\mu}$ is given by $\hat{\mu} = \mu_n - \mu_p = \mu_e$ where μ_p , μ_n and μ_e are the chemical potentials of the protons, neutrons and electrons respectively. The stability of the uniform phase requires that $u(v, q)$ is a convex function [26]. This condition leads to the following two constraints for the pressure and the chemical potential

$$-\left(\frac{\partial P}{\partial v}\right)_q - \left(\frac{\partial P}{\partial q}\right)_v \left(\frac{\partial q}{\partial v}\right)_{\hat{\mu}} > 0, \quad (8)$$

$$-\left(\frac{\partial \hat{\mu}}{\partial q}\right)_v > 0. \quad (9)$$

It is assumed that the total internal energy per baryon $u(v, q)$ can be decomposed into baryon (E_N) and electron (E_e) contributions

$$u(v, q) = E_N(v, q) + E_e(v, q). \quad (10)$$

The related theory has been extensively presented in our recent publication [20]. We consider the condition of charge neutrality $q = 0$ which requires that $x = Y_e$. This is the case we will consider also in the present study. Hence, according to Ref. [20] the constraints (8) and (9), in the case of the full EOS (FEOS) and the parabolic approximation (PA), are written

$$C_{\text{FEOS}}(n) = 2n \frac{\partial E(n, x)}{\partial n} + n^2 \frac{\partial^2 E(n, x)}{\partial n^2} - \left(\frac{\partial^2 E(n, x)}{\partial n \partial x} n\right)^2 \left(\frac{\partial^2 E(n, x)}{\partial x^2}\right)^{-1} > 0, \quad (11)$$

$$C_{\text{PA}}(n) = n^2 \frac{d^2 E(n, x=0.5)}{dn^2} + 2n \frac{dE(n, x=0.5)}{dn} + (1-2x)^2 \times \left[n^2 \frac{d^2 E_{\text{sym}}(n)}{dn^2} + 2n \frac{dE_{\text{sym}}(n)}{dn} - 2 \frac{1}{E_{\text{sym}}(n)} \left(n \frac{dE_{\text{sym}}(n)}{dn} \right)^2 \right] > 0. \quad (12)$$

For a given equation of state, the quantity $C_{\text{FEOS}}(n)$ (or $C_{\text{PA}}(n)$) is plotted as a function of the baryonic density n and the equation $C_{\text{FEOS}}(n) = 0$ (or $C_{\text{PA}}(n) = 0$) defines the transition density n_t . However, what remains is the determination of the proton fraction x (as a function of the baryon density n) in β -stable matter. In this case we have the processes

$$n \longrightarrow p + e^- + \bar{\nu}_e \qquad p + e^- \longrightarrow n + \nu_e \qquad (13)$$

which take place simultaneously. We assume that neutrinos generated in these reactions have left the system. This implies that

$$\hat{\mu} = \mu_n - \mu_p = \mu_e, \qquad (14)$$

Given the total energy density of the baryons $\epsilon_N \equiv \epsilon(n_n, n_p)$, the neutron and proton chemical potentials can be defined as (see also Ref. [27])

$$\mu_n = \left(\frac{\partial \epsilon_N}{\partial n_n} \right)_{n_p}, \qquad \mu_p = \left(\frac{\partial \epsilon_N}{\partial n_p} \right)_{n_n}. \qquad (15)$$

It is easy to show that after some algebra we get

$$\hat{\mu} = \mu_n - \mu_p = - \left(\frac{\partial(\epsilon_N/n)}{\partial x} \right)_n = \left(- \frac{\partial E_N}{\partial x} \right)_n. \qquad (16)$$

The charge condition implies that $n_e = n_p = nx$ or $k_{F_e} = k_{F_p}$ (where k_F are the fermi momenta). In addition, the chemical potential of the electron is given by the relation (relativistic electrons)

$$\mu_e = \sqrt{k_{F_e}^2 c^2 + m_e^2 c^4} \simeq k_{F_e} c = \hbar c (3\pi^2 nx)^{1/3}. \qquad (17)$$

Finally, from equations (16) and (17) one has

$$\left(\frac{\partial E_N}{\partial x} \right)_n = -\hbar c (3\pi^2 nx)^{1/3}. \qquad (18)$$

Equation (18) is the most general relation that determines the proton fraction of β -stable matter. In the case of the PA the above equation, with the help of Eq. (5) is written as

$$4(1 - 2x)E_{\text{sym}}(n) = \hbar c (3\pi^2 n_e)^{1/3} = \hbar c (3\pi^2 nx)^{1/3}. \qquad (19)$$

The pressure P_t at the inner edge is an important quantity directly related to the crustal fraction of the moment of inertia, which can be measured indirectly from observations of pulsars glitches [3]. The total pressure is decomposed also into baryon and lepton contributions

$$P(n, x) = P_N(n, x) + P_e(n, x), \qquad (20)$$

where

$$P_N(n, x) = n^2 \frac{\partial E_N}{\partial n}. \quad (21)$$

The electrons are considered as a non-interacting Fermi gas. Their contribution to the total pressure reads

$$P_e(n, x) = \frac{1}{12\pi^2} \frac{\mu_e^4}{(\hbar c)^3} = \frac{\hbar c}{12\pi^2} (3\pi^2 x n)^{4/3}. \quad (22)$$

The transition pressure, in the case of the FEOS, is given now by the equation

$$P_t^{FEOS}(n_t, x_t) = n_t^2 \left. \frac{\partial E_N}{\partial n} \right|_{n=n_t} + \frac{\hbar c}{12\pi^2} (3\pi^2 x_t n_t)^{4/3}, \quad (23)$$

where x_t is the proton fraction related to the transition density. In the case of the PA P_t is given by the relation

$$\begin{aligned} P_t^{PA}(n_t, x_t) &= n_t^2 \left(\left. \frac{dE(n, x=0.5)}{dn} \right|_{n=n_t} + \left. \frac{dE_{sym}(n)}{dn} \right|_{n=n_t} (1-2x_t)^2 \right) \\ &+ \frac{\hbar c}{12\pi^2} (3\pi^2 x_t n_t)^{4/3}. \end{aligned} \quad (24)$$

A. Application I: crustal fraction of the moment of inertia

The crustal fraction of the moment of inertia $\Delta I/I$ can be expressed as a function of M (star's total mass) and R (star's radius) with the only dependence on the equation of state arising from the values of P_t and n_t . Actually, the major dependence is on the value of P_t , since n_t enters only as a correction according to the following approximate formula [28]

$$\frac{\Delta I}{I} \simeq \frac{28\pi P_t R^3}{3Mc^2} \frac{(1 - 1.67\beta - 0.6\beta^2)}{\beta} \left(1 + \frac{2P_t}{n_t mc^2} \frac{(1 + 7\beta)(1 - 2\beta)}{\beta^2} \right)^{-1}, \quad (25)$$

where $\beta = GM/Rc^2$. The crustal fraction of the moment of inertia is particularly interesting as it can be inferred from observations of pulsar glitches, the occasional disruptions of the otherwise extremely regular pulsations from magnetized, rotating neutron stars [12]. Link et al. [28] showed that glitches represent a self-regulating instability for which the star prepares over a waiting time. The angular momentum requirements of glitches in the Vela pulsar indicate that more than 0.014 of the star's moment of inertia drives these events. So, if glitches originate in the liquid of the inner crust, this means that $\Delta I/I > 0.014$

B. Application II: r-mode instability of rotating neutron star

The r-modes are oscillations of rotating stars whose restoring force is the Coriolis force [29–40]. The gravitational radiation-driven instability of these modes has been proposed as an explanation for the observed relatively low spin frequencies of young neutron stars and of accreting neutron stars in low-mass X-ray binaries as well. This instability can only occur when the gravitational-radiation driving time scale of the r-mode is shorter than the time scales of the various dissipation mechanisms that may occur in the interior of the neutron star.

The nuclear EOS affects the time scales associated with the r-mode, in two different ways. Firstly, EOS defines the radial dependence of the mass density distribution $\rho(r)$, which is the basic ingredient of the relevant integrals. Secondly, it defines the core-crust transition density ρ_c and also the core radius R_c which is the upper limit of the mentioned integrals.

The critical angular velocity Ω_c , above which the r-mode is unstable, for $m = 2$ is given by [29]

$$\frac{\Omega_c}{\Omega_0} = \left(\frac{\tilde{\tau}_{GR}}{\tilde{\tau}_v} \right)^{2/11} \left(\frac{10^8 K}{T} \right)^{2/11}. \quad (26)$$

where $\Omega_0 = \sqrt{\pi G \bar{\rho}}$ and $\bar{\rho} = 3M/4\pi R^3$ is the mean density of the star and T is the temperature. $\tilde{\tau}_{GR}$ and $\tilde{\tau}_v$ are the fiducial gravitational radiation time scale and the fiducial viscous time scale respectively given by

$$\tau_{GR} = \tilde{\tau}_{GR} \left(\frac{\Omega_0}{\Omega} \right)^{2m+2}, \quad (27)$$

$$\tau_v = \tilde{\tau}_v \left(\frac{\Omega_0}{\Omega} \right)^{1/2} \left(\frac{T}{10^8 K} \right), \quad (28)$$

where [29]

$$\frac{1}{\tau_{GR}} = -\frac{32\pi G \Omega^{2m+2}}{c^{2m+3}} \frac{(m-1)^{2m}}{[(2m+1)!!]^2} \left(\frac{m+2}{m+1} \right)^{2m+2} \int_0^{R_c} \rho(r) r^{2m+2} dr, \quad (29)$$

and

$$\tau_v = \frac{1}{2\Omega} \frac{2^{m+3/2} (m+1)!}{m(2m+1)!! \mathcal{I}_m} \sqrt{\frac{2\Omega R_c^2 \rho_c}{\eta_c}} \int_0^{R_c} \frac{\rho(r)}{\rho_c} \left(\frac{r}{R_c} \right)^{2m+2} \frac{dr}{R_c}. \quad (30)$$

Ω is the angular velocity of the unperturbed star, $\rho(r)$ is the radial dependence of the mass density of the neutron star, R_c , ρ_c and η_c are the radius, density and viscosity of the fluid at the outer edge of the core. In the present work we consider the case of $m = 2$ r-mode.

IV. THE MODELS

In the present work we employ three different phenomenological models for the energy per baryon of the asymmetric nuclear matter having the advantage of an analytical form. The MDI model has been extensively applied for neutron star studies, can reproduce the results of more microscopic calculations of dense matter at zero temperature and can be extended to finite temperature [41–46]. The Skyrme model using various parametrizations can also be applied both in nuclear matter and in finite nuclei [47, 48]. Finally we employ a version of the Thomas-Fermi model, which was introduced by Myers *et al.* [49] and has also been applied for the study of finite nuclei and in a few cases for high density nuclear matter applications [50].

A. MDI model

The model used here, which has already been presented and analyzed in previous papers [41–46], is designed to reproduce the results of the microscopic calculations of both nuclear and neutron-rich matter at zero temperature and can be extended to finite temperature [41]. The energy density of the asymmetric nuclear matter (ANM), in MDI model is given by the relation

$$\epsilon(n_n, n_p, T = 0) = \epsilon_{kin}^n(n_n, T = 0) + \epsilon_{kin}^p(n_p, T = 0) + V_{int}(n_n, n_p, T = 0), \quad (31)$$

where the first two terms are the kinetic energy contributions on the total energy density, while the third one is the potential energy contribution. The energy per baryon at $T = 0$, is given by

$$\begin{aligned} E(n, I) = & \frac{3}{10} E_F^0 u^{2/3} [(1+I)^{5/3} + (1-I)^{5/3}] + \frac{1}{3} A \left[\frac{3}{2} - \left(\frac{1}{2} + x_0 \right) I^2 \right] u \\ & + \frac{\frac{2}{3} B \left[\frac{3}{2} - \left(\frac{1}{2} + x_3 \right) I^2 \right] u^\sigma}{1 + \frac{2}{3} B' \left[\frac{3}{2} - \left(\frac{1}{2} + x_3 \right) I^2 \right] u^{\sigma-1}} \\ & + \frac{3}{2} \sum_{i=1,2} \left[C_i + \frac{C_i - 8Z_i}{5} I \right] \left(\frac{\Lambda_i}{k_F^0} \right)^3 \left(\frac{((1+I)u)^{1/3}}{\frac{\Lambda_i}{k_F^0}} - \tan^{-1} \frac{((1+I)u)^{1/3}}{\frac{\Lambda_i}{k_F^0}} \right) \\ & + \frac{3}{2} \sum_{i=1,2} \left[C_i - \frac{C_i - 8Z_i}{5} I \right] \left(\frac{\Lambda_i}{k_F^0} \right)^3 \left(\frac{((1-I)u)^{1/3}}{\frac{\Lambda_i}{k_F^0}} - \tan^{-1} \frac{((1-I)u)^{1/3}}{\frac{\Lambda_i}{k_F^0}} \right). \end{aligned} \quad (32)$$

In Eq. (32), I is the asymmetry parameter ($I = (n_n - n_p)/n$) and $u = n/n_0$, with n_0 denoting the equilibrium symmetric nuclear matter density, $n_0 = 0.16 \text{ fm}^{-3}$. The parameters A , B , σ , C_1 , C_2 and B' which appear in the description of symmetric nuclear matter are determined in order that $E(n = n_0) - mc^2 = -16 \text{ MeV}$, $n_0 = 0.16 \text{ fm}^{-3}$, and the incompressibility is $K = 240 \text{ MeV}$ and have the values $A = -46.65$, $B = 39.45$, $\sigma = 1.663$, $C_1 = -83.84$, $C_2 = 23$ and $B' = 0.3$. The finite range parameters are $\Lambda_1 = 1.5k_F^0$ and $\Lambda_2 = 3k_F^0$ and k_F^0 is the Fermi momentum at the saturation point n_0 .

TABLE I: The parameters for neutron rich matter of MDI model.

$F(u)$	x_0	x_3	Z_1	Z_3
\sqrt{u}	0.376	0.246	-12.23	-2.98
u	0.927	-0.227	-11.51	8.38
$2u^2/(1+u)$	1.654	-1.112	3.81	13.16

The additional parameters x_0 , x_3 , Z_1 , and Z_2 employed to determine the properties of asymmetric nuclear matter are treated as parameters constrained by empirical knowledge [41] and presented in Table 1. By suitably choosing the parameters x_0 , x_3 , Z_1 , and Z_2 , it is possible to obtain different forms for the density dependence of the symmetry energy $E_{sym}(u)$. The nuclear symmetry energy is parametrized according to the following formula

$$E_{sym}(n) = 13u^{2/3} + 17F(u), \quad (33)$$

where the first term of the right-hand side of Eq. (33) represents the contribution of the kinetic energy and the second term is the contribution of the interaction energy. In general, in order to obtain different forms for the density dependence of $E_{sym}(n)$, the function $F(u)$ can be parameterized as follows [41]

$$F(u) = \sqrt{u}, \quad F(u) = u, \quad F(u) = 2u^2/(1+u). \quad (34)$$

In the present work its parametrization corresponds to the models MDI-1, MDI-2 and MDI-3 respectively. Numerical values of the parameters that generate these functional forms are given in Table 1. It is worthwhile to point out that the above parametrization of the

interaction part of the nuclear symmetry energy is extensively used for the study of neutron star properties [27, 41] as well as the study of the collisions of neutron-rich heavy ions at intermediate energies [51, 52].

The pressure of the baryons, at $T = 0$, defined as

$$P = n^2 \frac{\partial E(n, I)}{\partial n}, \quad (35)$$

with the help of Eq. (32) takes the analytical form

$$\begin{aligned} P(n, I) = & \frac{1}{5} n_0 E_F^0 u^{5/3} [(1+I)^{5/3} + (1-I)^{5/3}] + \frac{1}{3} n_0 u^2 A \left[\frac{3}{2} - \left(\frac{1}{2} + x_0 \right) I^2 \right] \\ & + \frac{2}{3} B \sigma n_0 u^{\sigma+1} \frac{\left[\frac{3}{2} - \left(\frac{1}{2} + x_3 \right) I^2 \right] \left(1 + \frac{2}{3\sigma} B' u^{\sigma-1} \left[\frac{3}{2} - \left(\frac{1}{2} + x_3 \right) I^2 \right] \right)}{\left(1 + \frac{2}{3} B' \left[\frac{3}{2} - \left(\frac{1}{2} + x_3 \right) I^2 \right] u^{\sigma-1} \right)^2} \\ & + \frac{n_0 u^2}{2} \sum_{i=1,2} \left[C_i + \frac{C_i - 8Z_i}{5} I \right] \left(\frac{\Lambda_i}{k_F^0} \right)^2 \frac{(1+I)^{1/3}}{u^{2/3}} \left(1 - \frac{1}{1 + \frac{(1+I)^{2/3} u^{2/3}}{\left(\frac{\Lambda_i}{k_F^0} \right)^2}} \right) \\ & + \frac{n_0 u^2}{2} \sum_{i=1,2} \left[C_i - \frac{C_i - 8Z_i}{5} I \right] \left(\frac{\Lambda_i}{k_F^0} \right)^2 \frac{(1-I)^{1/3}}{u^{2/3}} \left(1 - \frac{1}{1 + \frac{(1-I)^{2/3} u^{2/3}}{\left(\frac{\Lambda_i}{k_F^0} \right)^2}} \right). \end{aligned} \quad (36)$$

B. Skyrme model

The Skyrme functional providing the energy per baryon of asymmetric nuclear matter is given by the formula [47, 48]

$$\begin{aligned} E(n, I) = & \frac{3}{10} \frac{\hbar^2 c^2}{m} \left(\frac{3\pi^2}{2} \right)^{2/3} n^{2/3} F_{5/3}(I) + \frac{1}{8} t_0 n [2(x_0 + 2) - (2x_0 + 1)F_2(I)] \\ & + \frac{1}{48} t_3 n^{\sigma+1} [2(x_3 + 2) - (2x_3 + 1)F_2(I)] \\ & + \frac{3}{40} \left(\frac{3\pi^2}{2} \right)^{2/3} n^{5/3} \left[(t_1(x_1 + 2) + t_2(x_2 + 2)) F_{5/3}(I) \right. \\ & \left. + \frac{1}{2} (t_2(2x_2 + 1) - t_1(2x_1 + 1)) F_{8/3}(I) \right], \end{aligned} \quad (37)$$

where $F_m(I) = \frac{1}{2} [(1+I)^m + (1-I)^m]$ and the parametrization is given in Refs [47, 48].

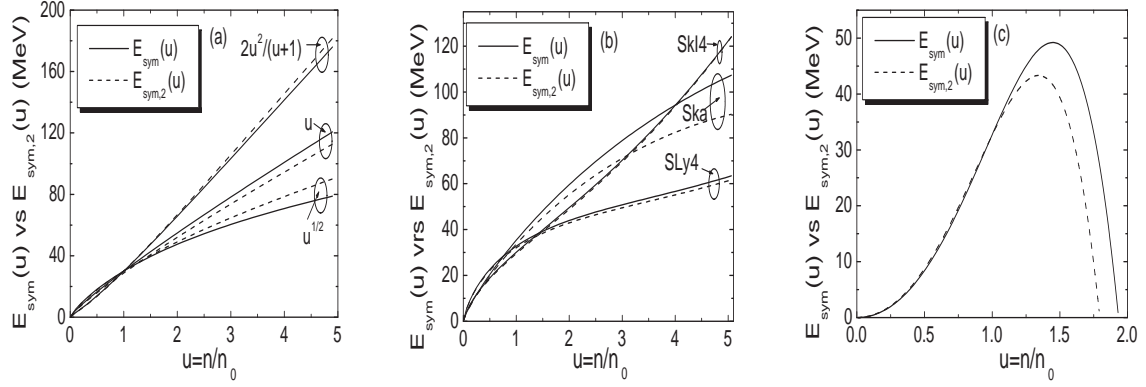


FIG. 1: The symmetry energy $E_{sym}(u)$ defined by Eq. (4) versus the symmetry energy $E_{sym,2}(u)$ defined by Eq. (2) as a function of the density fraction $u = n/n_0$ for the three considered models.

C. Thomas-Fermi model

The model's prediction for the equation of state reads $E(n, I) = T_0 \eta(u, I)$, where [49]

$$\eta(u, I) = a(I)\Omega^3 - b(I)\Omega^3 + c(I)\Omega^5, \quad \Omega \equiv (n/n_0)^{1/3}, \quad n_0 = 0.16114 \text{ fm}^{-3} \quad (38)$$

n_0 and T_0 are the saturation density and Fermi energy of standard nuclear matter accordingly as predicted by the model and the coefficients $a(I)$, $b(I)$, $c(I)$ are the following functions of I

$$a(I) = \frac{3}{20} \left[2(1 - \gamma_l)(p^5 + q^5) - \gamma_u \begin{cases} (5p^2q^3 - q^5) & \text{for } n_n \geq n_p \\ (5p^3q^2 - p^5) & \text{for } n_n \leq n_p \end{cases} \right], \quad (39)$$

$$b(I) = \frac{1}{4} [\alpha_l(p^6 + q^6) + 2\alpha_u p^3 q^3], \quad (40)$$

$$c(I) = \frac{3}{10} [B_l(p^8 + q^8) + B_u p^3 q^3 (p^2 + q^2)], \quad (41)$$

where $p = (1 + I)^{1/3}$, $q = (1 - I)^{1/3}$. The interaction strengths $\gamma_l, \gamma_u, \alpha_l, \alpha_u, B_l, B_u$ have the following values: $\gamma_l = 0.25198$, $\gamma_u = 0.88474$, $\alpha_l = 0.7011$, $\alpha_u = 1.24574$, $B_l = 0.22791$, $B_u = 0.8002$.

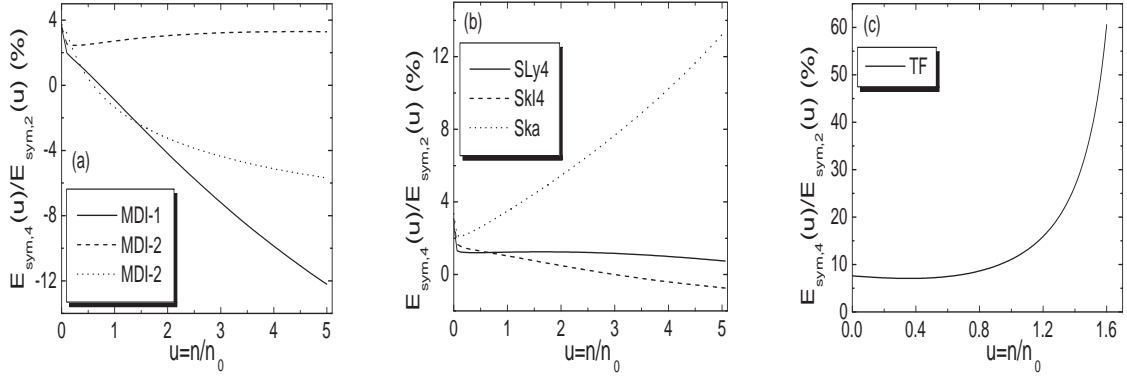


FIG. 2: The density dependence of the ratio $E_{sym,4}(u)/E_{sym,2}(u)$ for the three considered models.

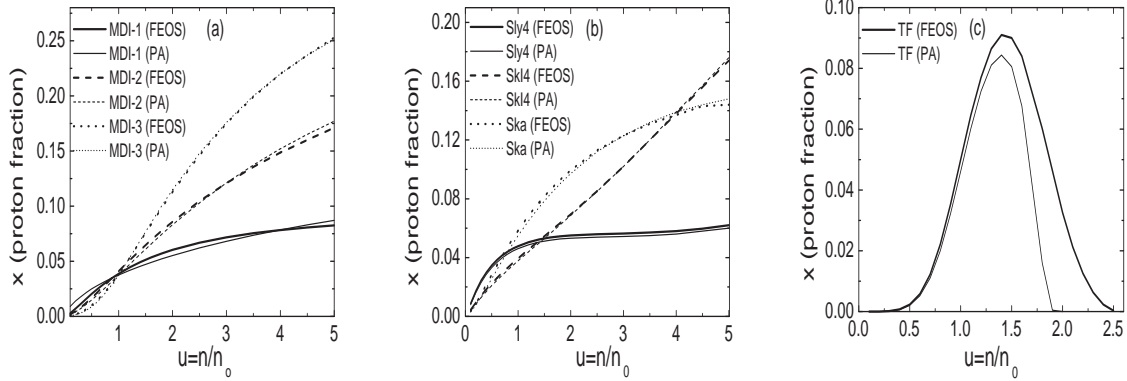


FIG. 3: The density dependence of the proton fraction x obtained from the considered models employing the FEOS as well as the PA.

V. RESULTS AND DISCUSSION

In Fig. 1 we compare the density dependence of the quantities $E_{sym,2}(n) = \frac{1}{2!} \frac{\partial^2 E(n, I)}{\partial I^2} \Big|_{I=0}$ and $E_{sym}(n) = E(n, I = 1) - E(n, I = 0)$. Both definitions of the symmetry energy exhibit a similar behavior for low values of the baryon density (up to $u \simeq 1.5$). The difference, which is model dependent, is more pronounced for higher values of n . This is a direct indication that the two approaches affect the equation of state of high density nuclear matter at the inner core of neutron stars. It is worth noticing that for the three MDI models and the three Skyrme models the symmetry energy is an increasing function of the density.

In TF model the symmetry energy is increasing as a function of u only up to $u \simeq 1.5$ and then decreases rapidly with u . This has a dramatic effect on neutron stars applications mainly on those connected with the high density equation of state.

In order to check the accuracy of the parabolic approximation we display in Fig. 2 the density dependence of the ratio $E_{sym,4}(u)/E_{sym,2}(u)$. It is seen that in most cases the contribution of the fourth-order term $E_{sym,4}(u)$ is less than 4% compared to the second order one $E_{sym,2}(u)$, at least for low values of the density ($u \leq 2$). However, in four of the considered models, i.e. the MDI-1, MDI-3, the SKa and TF the contribution of $E_{sym,4}(u)$ increases rapidly with the density and consequently influences the high density equation of state and this must be taken into account. In the specific case of the TF model the contribution of $E_{sym,4}(u)$ becomes comparable to $E_{sym,2}(u)$ even for low values of u , making the parabolic approximation problematic.

In Fig. 3 we compare the density dependence of proton fraction x in β -stable nuclear matter determined by employing the full EOS (FEOS) and the parabolic approximation. In the case of the MDI and Skyrme models there is a difference (depending on the specific model) mainly between 4% and 20% for low values of the baryon density (up to $u \simeq 0.7$). However, the parabolic approximation is good for higher values of n . We expect that the above density dependence of x will be reflected also on the values of the transition density n_t and pressure P_t . In the case of the TF model only for low values of the density ($u \leq 1$) the two approximations produce similar results. Moreover, it is concluded that the parabolic approximation does not affect appreciably the onset of the URCA process with critical values $x_{URCA} \simeq 11\%$ (without muons) and $x_{URCA} \simeq 14\%$ by including muons.

In Fig. 4(a), we present the correlation between the derivative of the symmetry energy $E_{sym,2}(n)$ (for $n = 1/2n_0$, $n = n_0$ and $n = 3/2n_0$) for the MDI and Skyrme models and the transition density n_t in the case of the FEOS. The most distinctive feature is the concentration of the data from the case $n = 1/2n_0$ (where they are rather random) to an almost linear relation in the case $n = n_0$ and linear in the case $n = 3/2n_0$. To further illustrate this point, we plot in Fig. 5 the derivative of the symmetry energy $E'_{sym,2}(n)$ at the baryon density $n = 3n_0/2$ versus n_t . A linear relation is found of the form

$$E'_{sym,2} \left(n = \frac{3n_0}{2} \right) = 400.18 - 3483.3n_t, \quad (\text{MeV} \cdot \text{fm}^3). \quad (42)$$

We find that the values of n_t depend on the trend of the equation of state and the symmetry

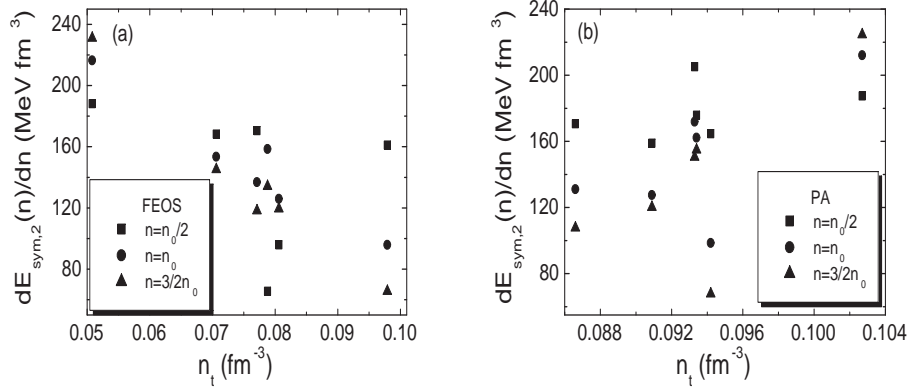


FIG. 4: The derivative of the symmetry energy $dE_{sym,2}(n)/dn$ versus the transition density n_t corresponding to the considered models a) employing the full EOS and b) employing the parabolic approximation.

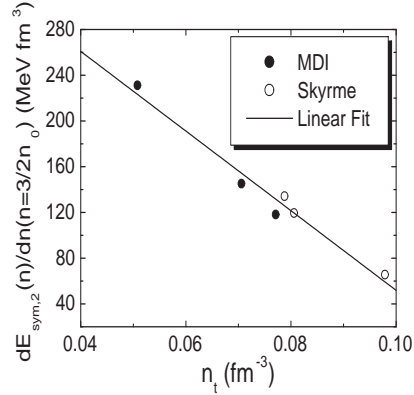


FIG. 5: The derivative of the symmetry energy $dE_{sym,2}(n = 3/2n_0)/dn$ versus the transition density, for the FEOS, corresponding to the considered models. The solid line corresponds to the least-squares fit (FIT) expression (42).

energy depends not only on values close to the saturation density n_0 but even on higher ones. It is of interest to see that, according to Fig. 4(b) in the case of the PA the data are scattered even for values close to $n = 3/2n_0$. It is presumed that the use of the PA may affect the linear correlation between $E'_{sym,2}(n)$ and n_t for $n = 3/2n_0$.

In Table 2 we present the values of n_t and P_t determined by employing the FEOS and

TABLE II: The transition density n_t (in fm^{-3}) and pressure P_t (in MeV) obtained from the considered models by employing the FEOS as well as the parabolic approximation.

approach	MDI-1	MDI-2	MDI-3	TF	Sly4	SKI4	Ska
n_t (FEOS)	0.0771	0.0706	0.0508	0.1368	0.0979	0.0806	0.0788
n_t (PA)	0.0866	0.0934	0.1027	0.1419	0.0942	0.0909	0.0933
P_t (FEOS)	0.3456	0.2338	0.3133	2.9020	0.5781	0.3365	0.5295
P_t (PA)	0.2975	0.7055	1.2482	3.7300	0.5459	0.4965	0.8651

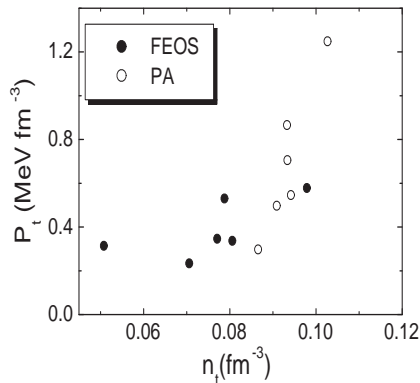


FIG. 6: The transition pressure P_t versus the transition density n_t employing the full and the parabolic approximation.

the parabolic approximation for the models considered in the present work. In most of the cases (the only exception is the Sly4 case) the use of the PA increases the values of n_t by 10-15 % or even more (see the case MDI-3). The effect of the PA is even more dramatic in the case of P_t . In most of the cases P_t increases significantly compared to the FEOS (the only exceptions are the MDI-1 and the Sly4 models). The increase is even two or three times. In order to clarify further this point we plot in Fig. 6 the values of P_t versus n_t for the considered models. We see the strong dependence of P_t on n_t in the case of PA compared to FEOS. The above results indicate that one may introduce a large error by employing the parabolic approximation in order to determine the value of P_t .

The values of P_t , according to Eq. (25), strongly influence the value of the crustal fraction of the moment of inertia. Actually, the crustal fraction $\Delta I/I$ depends not only on P_t and n_t but on the mass M and radius of R of the neutron star as well. Actually M and R depend also on P_t and n_t . In order to have a qualitative picture of the effect of P_t and n_t on $\Delta I/I$ we can consider the maximum mass and the corresponding radius R of the neutron star coming from the MDI model [53] and neglecting the effects of P_t and n_t (which is a good approximation). We determine the ratio $\Delta I/I$ by considering the full EOS and the parabolic approximation. The results are presented in Table 3. Its obvious that there is a strong difference between of two approaches. For example in the case of MDI-2 the PA increases more than two times the value of $\Delta I/I$ compared to the FEOS, while in the case of MDI-3 the increase is even higher.

TABLE III: The crustal fraction of the moment of inertia for the three MDI models employing the FEOS as well as the parabolic approximation.

Model	M_{max}/M_{\odot}	$R(Km)$	$\Delta I/I(\text{FEOS})$	$\Delta I/I(\text{PA})$
MDI-1	1.895	10.112	0.0076	0.0068
MDI-2	1.935	10.570	0.0062	0.0163
MDI-3	1.952	10.933	0.0086	0.0287

The limit $\Delta I/I = 0.014$ constrained by Link *et al.* [28] limits also the masses and the radii of the neutron star for specific values of P_t and n_t . It is concluded that the strong dependence of $\Delta I/I = 0.014$ on P_t puts also strong constraints on the allowed pairs of M and R . In Fig. 7 we plot the M-R constrained relation for the Vela pulsar where $\Delta I/I > 0.014$ obtained from the full and parabolic approximation in the case of the MDI model and the Skyrme model. It is obvious that the implication of the full EOS imposes more restrictive constraints compared to the parabolic one. This effect is more pronounced in the case of the MDI models compared to Skyrme model. Consequently, the use of the PA may also introduce a large error in the determination of the minimum radius (for a fixed value of a mass) of a neutron star.

In Fig. 8 we compare the r-mode instability window, obtained from the FEOS and PA in the case of the MDI model, with those of the observed neutron stars in low-mass x-ray

binaries (LMXBs) for $M = 1.4M_{\odot}$. The critical frequencies are strongly localized at high values in the case of the PA. The employment of the FEOS drops significantly the instability window, especially in the case of the stiffer equation of state (MDI-3 case). More specifically, the employment of the FEOS comparing to PA decreases the values of the critical frequency ν_c around 4% (MDI-1), 8% (MDI-2) and 24% (MDI-3).

In addition, following the study of Wen *et al.* [38] we examine four cases of LMXBs that is the 4U 1608-522 at 620 Hz, 4U 1636-536 at 581 Hz, MXB 1658-298 at 567 Hz and EXO 0748-676 at 552 Hz [54, 55]. The masses of the mentioned stars are not measured accurately but the core temperature T is derived from their observed accretion luminosity. It is obvious from Fig. 8 that for a $M = 1.4M_{\odot}$ three of the considered LMXBs lie inside instability window. According to discussion of Ref. [38] and finding in Refs. [56, 57] the LMXBs should be out of the instability window. Consequently, one can presume that either the LMXBs masses are even lower than $M = 1.4M_{\odot}$ or the softer equation of state is more preferred. However, additional theoretical and observation work must be dedicated before a definite conclusion.

VI. SUMMARY

The study of symmetry energy effects on location of the inner edge of neutron star crusts is the main topic of the present work. We employ three different phenomenological models for the prediction of the EOS and we determine in the framework of thermodynamical method both the transition density and transition pressure corresponding to the inner edge of a neutron star crust. Actually, n_t and P_t have been determined separately by employing the full equation of state of asymmetric matter and its parabolic approximation. Our results confirm the statement that employing the PA instead of the full EOS may influence appreciably the values of n_t and even more the values of P_t . We found that there is a linear correlation between the derivative of the symmetry energy $E'_{sym,2}(n)$ at the baryon density $n = 3n_0/2$ and the transition density n_t for the considered models. We found also that the implication of the full EOS imposes more restrictive constraints, on the M-R constrained relation for the Vela pulsar, compared to the parabolic one. Furthermore, the employment of the FEOS drops significantly the instability window, especially in the case of the stiff equation of state.

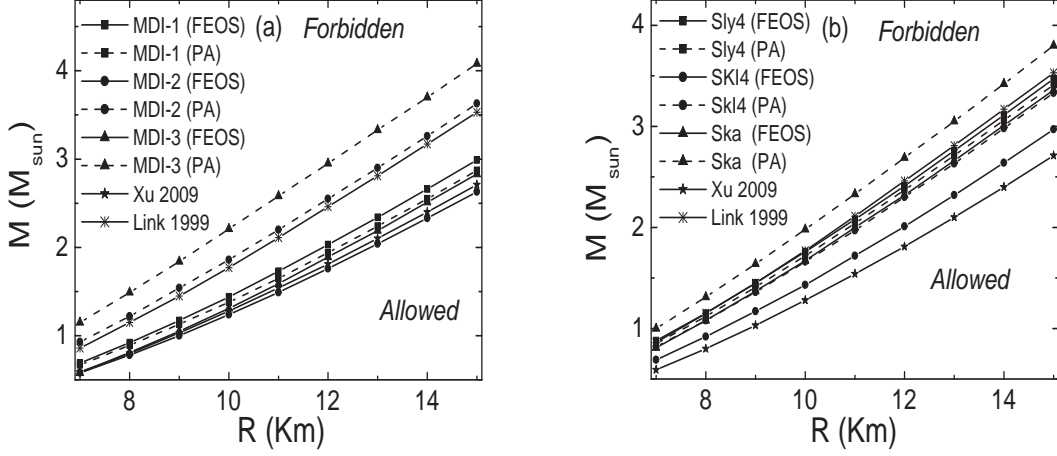


FIG. 7: The M-R constrained relation for the Vela pulsar where $\Delta I/I > 0.014$ obtained from the FEOS and PA in the case of a) the MDI model and b) the Skyrme model. The constraint implies that allowed masses (in M_{\odot}) and radii lie to the right of the line. The two additional constraints are taken from Xu *et al.* [11] ($n_t = 0.065 \text{ fm}^{-3}$ and $P_t = 0.26 \text{ MeV fm}^{-3}$) and Link *et al.* [28] ($n_t = 0.075 \text{ fm}^{-3}$ and $P_t = 0.65 \text{ MeV fm}^{-3}$).

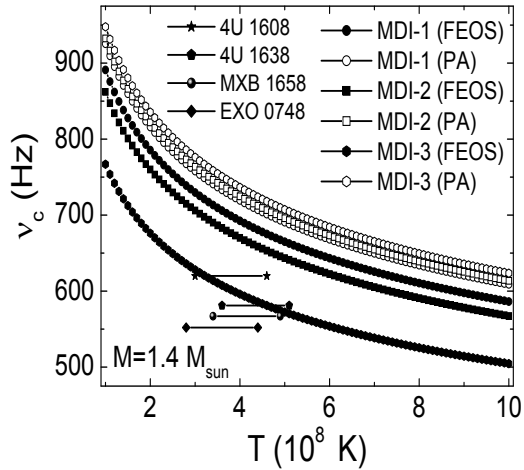


FIG. 8: The critical frequency temperature dependence for a neutron star with mass $M = 1.4M_{\odot}$ obtained from the FEOS and PA in the case of the MDI model. In addition, the location of the observed short-recurrence-time LMXBs [54, 55].

Consequently, the error introduced by assuming that EOS is parabolic may induce also a large error in the determination of related properties of a neutron star as the crustal fraction on the moment of inertia and the critical frequency of rotating neutron stars.

Acknowledgments

This work was supported by the German Science Council (DFG) via SFB/TR7. The author would like to thank the Theoretical Astrophysics Department of the University of Tuebingen, where part of this work was performed and Professor K. Kokkotas for his useful comments on the preparation of the manuscript. The author thanks Dr. C.P. Panos for his remarks on the present paper.

-
- [1] S.L. Shapiro and S.A. Teukolsky, *Black Holes, White Dwarfs, and Neutron Stars* (John Wiley and Sons, New York, 1983).
 - [2] P. Haensel, A.Y. Potekhin, and D.G. Yakovlev, *Neutron Stars 1: Equation of State and Structure* (Springer-Verlag, New York, 2007).
 - [3] J.M. Lattimer and M. Prakash, Phys. Rep. **442**, 109 (2007).
 - [4] C.J. Pethick, D.G. Ravenhall, and C.P. Lorenz, Nucl. Phys. A **584**, 675 (1995).
 - [5] G. Baym, C. Pethick, and P. Sutherland, Astrophys. J. **170**, 299 (1971).
 - [6] G. Baym, H. A. Bethe, and C.J. Pethick, Nucl. Phys. A **175**, 225 (1971).
 - [7] C.J. Pethick and D.G. Ravenhall, Ann. Rev. Nucl. Part. Sci. **45**, 429 (1995).
 - [8] F. Douchin and P. Haensel, Phys. Let. B **485**, 107 (200).
 - [9] K. Oyamatsu and K. Iida, Phys. Rev. C **75**, 015801 (2007).
 - [10] C. Ducoin, Ph. Chomaz, and F. Gulminelli, Nucl. Phys. A **789**, 403 (2007).
 - [11] J. Xu, L.W. Chen, B.A. Li, and H.R. Ma, Phys. Rev. C **79**, 035802 (2009).
 - [12] J. Xu, L.W. Chen, B.A. Li, and H.R. Ma, Astrophys. J. **697**, 1549 (2009).
 - [13] S. Kubis, Phys. Rev. C **76**, 025801 (2007).
 - [14] A. Worley, P.G. Krastev, and B.A. Li, Astrophys. J. **685**, 390 (2008).
 - [15] S. Kubis, Phys. Rev. C **70**, 065804 (2004).

- [16] C.J. Horowitz and J. Piekarewicz, Phys. Rev. Lett. **86**, 5647 (2001).
- [17] J. Carriere, C.J. Horowitz, and J. Piekarewicz, Astrophys. J. **593**, 463 (2003).
- [18] C. Ducoin, J. Margueron, C. Providencia and I. Vidana, Phys. Rev. C **83**, 045810 (2011).
- [19] C. Ducoin, J. Margueron and C. Providencia, Eur. Phys. Lett. **91**, 32001 (2010).
- [20] Ch.C. Moustakidis, T. Nikšić, G.A. Lalazissis, D. Vretenar and P. Ring, Phys. Rev. C **81**, 065803 (2010).
- [21] J. Xu, L.W. Chen, C.M. Ko, and B.A. Li, Phys. Rev. C **81**, 055805 (2010).
- [22] B.J. Cai and L.W. Chen, Phys. Rev. C **85**, 024302 (2012).
- [23] B.A. Li, L.W. Chen, and C.M. Ko, Phys. Rep. **464**, 113 (2008).
- [24] M.B. Tsang et al., Phys. Rev. Lett. **92**, 062701(2004).
- [25] M.B. Tsang, Y. Zhang, P. Danielewicz, M. Famiano, Z. Li, W.G. Lynch, and A.W. Steiner, Phys. Rev. Lett. **102**, 122701 (2009).
- [26] H.B. Callen, Thermodynamics, Wiley, New York, 1985.
- [27] M. Prakash *The Equation of State and Neutron Star* lectures delivered at the Winter School held in Puri India 1994.
- [28] B. Link, R.I. Epstein, and J.M. Lattimer, Phys. Rev. Lett., **83**, 3362, (1999).
- [29] L. Lindblom, B.J. Owen, and G. Ushomirsky, Phys. Rev. D **62**, 084030 (2000).
- [30] N. Andersson, Astrophys. J. **502**, 708 (1998).
- [31] J.L. Friedman and S.M. Morsink, Astrophys. J. **502**, 714 (1998).
- [32] J.L. Friedman and K.H. Lockitch, Prog. Theor. Phys. Suppl. **136**, 121 (1999).
- [33] N. Andersson and K.D. Kokkotas, Int. J. Mod. Phys. D **10**, 381 (2001).
- [34] N. Andersson, Class. Quantum Grav. **20**, R105 (2003).
- [35] K.D. Kokkotas and N. Stergioulas, Astron. Astrophys. **341**, 110 (1999).
- [36] N. Andersson, K. Kokkotas, and B.F. Schutz, Astrophys. J. **510**, 846 (1999).
- [37] L. Bildsten and G. Ushomirsky, Astroph. J. Lett. **529**, L33 (2000).
- [38] D.H. Wen, W.G. Newton, and B.A. Li, Phys. Rev. C **85**, 025801 (2012).
- [39] I. Vidana, Phys. Rev. C **85**, 045808 (2012).
- [40] M.G. Alford, S. Mahmoodifar, and K. Schwenzer, Phys. Rev. D **85**, 024007 (2000).
- [41] Madappa Prakash, I. Bombaci, Manju Prakash, P.J. Ellis, J.M. Lattimer, R. Knorren, Phys. Rep. **280**, 1 (1997).

- [42] V.P. Psonis, Ch.C. Moustakidis, and S.E. Massen, *Mod. Phys. Let. A* **22**, 1233 (2007).
- [43] Ch.C. Moustakidis, *Phys. Rev. C* **76**, 025805 (2007).
- [44] Ch.C. Moustakidis, *Phys. Rev. C* **78**, 054323 (2008).
- [45] Ch.C. Moustakidis and C.P. Panos, *Phys. Rev. C* **79**, 045806 (2009).
- [46] Ch.C. Moustakidis, *Int. J. Mod. Phys. D*, **18**, 1205 (2009).
- [47] E. Chabanat, P. Bonche, P. Haensel, J. Meyer and R. Schaeffer, *Nucl. Phys. A* **627**, 710 (1997).
- [48] M. Farine, J.M. Pearson and F. Tondeur, *Nucl. Phys. A* **615**, 135 (1997).
- [49] W.D. Myers and W.J. Swiatecki, *Phys. Rev. C* **57**, 3020 (1998).
- [50] K. Strobel, F. Weber, M.K. Weigel and Ch. Schaab, *Int. J. Mod. Phys. E* **6**, 669 (1997).
- [51] B.A. Li, C.M. Ko and Z. Ren, *Phys. Rev. Lett.* **78**, 1644 (1997).
- [52] V. Baran, M. Colonna, V. Greco and M.Di Toro, *Phys. Rep.* **410**, 335 (2005).
- [53] M. Prakash, T.L. Ainworth and J.M. Lattimer, *Phys. Rev. Lett.*, **61**, 2518 (1988).
- [54] A.L. Watts, B. Krishnam, L. Bildsten, and B.F. Schutz, *Mon. Not. R. Astron. Soc.* **389**, 839 (2008).
- [55] L. Keek, D.K. Galloway, J.J. M. in't Zand, and A. Heger, *Astrophys. J.* **718**, 292 (2010).
- [56] Y. Levin, *Astrophys. J.* **517**, 328 (1999).
- [57] R. Bondarescu, S.A. Teukolsky, and I. Wasserman, *Phys. Rev. D* **76**, 064019 (2007).